HHS Public Access

Author manuscript

Am J Surg Pathol. Author manuscript; available in PMC 2020 November 01.

Published in final edited form as:

Am J Surg Pathol. 2019 November ; 43(11): 1445–1461. doi:10.1097/PAS.0000000000001307.

TFEB Expression Profiling in Renal Cell Carcinomas: Clinicopathologic Correlations

Sounak Gupta, MBBS, PhD[1], **Pedram Argani, MD**[2], **Achim A. Jungbluth, MD, PhD**[1], **Ying-Bei Chen, MD, PhD**[1], **Satish K. Tickoo, MD**[1], **Samson W. Fine, MD**[1], **Anuradha Gopalan, MD**[1], **Hikmat A. Al-Ahmadie, MD**[1], **Sahussapont J. Sirintrapun, MD**[1], **Alejandro Sanchez, MD**[3,4], **A. Ari Hakimi, MD**[3,4], **Tiffany Mcfarlane**[1], **Paulo A. Salazar**[1], **Sean R. Williamson, MD**[5], **Stephanie L. Skala, MD**[6], **Rohit Mehra, MD**[6], **Ondrej Hes, MD**[7], **Cristina R. Antonescu, MD**[1], **Marc Ladanyi, MD**[1], **Maria E. Arcila, MD**[1], **Victor E. Reuter, MD**[1]

[1]Department of Pathology, Memorial Sloan Kettering Cancer Center, New York, NY, USA;

[2]Department of Pathology, The Johns Hopkins Medical Institutions, Baltimore, MD, USA;

[3]Department of Surgery, Urology Service, Memorial Sloan Kettering Cancer Center, New York, NY, USA.

[4]Department of Human Oncology and Pathogenesis Program, Memorial Sloan Kettering Cancer Center, New York, NY, USA.

[5]Department of Pathology & Laboratory Medicine, Henry Ford Health System, Detroit, MI, US;

[6]Department of Pathology, University of Michigan Health System, Ann Arbor, MI, USA;

[7]Department of Pathology, University Hospital Plzeň, Charles University, Pilsen, Czech Republic.

Abstract

TFEB is overexpressed in *TFEB*-rearranged renal cell carcinomas as well as in renal tumors with amplifications of *TFEB* at 6p21.1. As recent literature suggests that renal tumors with 6p21.1 amplification behave more aggressively than those with rearrangements of *TFEB*, we compared relative *TFEB* gene expression in these tumors.

This study included 37 *TFEB*-altered tumors: 15 6p21.1-amplified and 22 *TFEB*-rearranged (including 5 cases from The Cancer Genome Atlas dataset). *TFEB* status was verified using a combination of FISH (n=27) or comprehensive molecular profiling (n=13) and digital droplet PCR was used to quantify *TFEB* mRNA expression in 6p21.1-amplified (n=9) and *TFEB*-rearranged renal tumors (n=19). These results were correlated with TFEB immunohistochemistry.

TFEB-altered tumors had higher *TFEB* expression when normalized to *B2M* (mean: 168.9%, n=28), compared to non-*TFEB*-altered controls (mean: 7%, n=18, p=0.005). Interestingly, *TFEB* expression in tumors with rearrangements (mean: 224.7%, n=19) was higher compared to 6p21.1-amplified tumors (mean: 51.2%, n=9; p=0.06). Of note, classic biphasic morphology was only seen in *TFEB*-rearranged tumors and when present correlated with 6.8-fold higher *TFEB* expression (p=0.00004).

Corresponding address for proof and reprints: Victor E. Reuter, MD, Department of Pathology, Memorial Sloan Kettering Cancer Center, 1275 York Avenue, New York, NY, 10065, Telephone: 212-639-8225, reuterv@mskcc.org.

Our results suggest that 6p21.1 amplified renal tumors show increased *TFEB* gene expression but not as much as t(6;11) renal tumors. These findings correlate with the less consistent/diffuse expression of downstream markers of *TFEB* activation (cathepsin K, melan A, HMB45) seen in the amplified neoplasms. This suggests that the aggressive biologic behavior of 6p21.1 amplified renal tumors might be secondary to other genes at the 6p21.1 locus that are co-amplified, such as *VEGFA* and *CCND3*, or other genetic alterations.

Keywords

TFEB; Renal Cell Carcinoma; 6p21.1 Amplification; Rearrangement

Introduction

Transcription Factor EB (*TFEB*), a member of the microphthalmia-associated transcription factor family, when overexpressed, is thought to act as a key oncogenic driver in renal cell carcinomas (1, 2). The mechanism of TFEB overexpression that was initially described in *TFEB*-driven renal tumors involved structural rearrangements such as t(6;11), where the complete *TFEB* coding sequence was retained in most cases (1, 3–5). Subsequently, genomic amplifications at the chromosome 6p21.1 locus were described where TFEB overexpression secondary to copy number increases emerged as an alternate pathogenic mechanism in *TFEB*-driven renal tumors (2, 6–12).

Recent studies have highlighted that 6p21.1 (*TFEB*) amplified tumors may be biologically distinct from *TFEB* rearranged tumors as 6p21.1-amplified tumors show amplification of other oncogenes at the same locus, such as *VEGFA* and *CCND3* (8, 9, 11, 12). In addition, initial reports suggest that the incidence of regional and distant metastasis in 6p21.1 (*TFEB*) amplified tumors may be higher than in *TFEB* rearranged tumors, which are thought to have a more indolent clinical course (2, 8, 9, 11–13).

The assessment of *TFEB* gene expression in these tumors has been pursued in a limited number of studies given that, until recently, the primary mechanism of *TFEB* overexpression, as a driver event, was thought to involve only gene rearrangements (5). Therefore, to better understand the pathogenesis of these tumors, *TFEB* gene expression status was assessed in both *TFEB* amplified and rearranged tumors. These results were then correlated with various clinicopathologic features including morphology, background genomic alterations and biologic behavior in a relatively large cohort of cases.

Materials and Methods

Patient Specimens

Six renal tumors with 6p21.1 (*TFEB*) amplifications, including 3 cases with *TFEB* rearrangements in the setting of a concurrent amplification at this locus, were identified from previously reported The Cancer Genome Atlas datasets (2, 8, 14, 15). This included an institutional case with *COL21A1-TFEB* rearrangement which was further characterized in this study (Figure 1).

This study was approved by the Memorial Sloan Kettering Cancer Center institutional review board and included cases that were profiled using a comprehensive molecular profiling strategy (Memorial Sloan Kettering Cancer Center Integrated Mutation Profiling of Actionable Cancer Targets (MSK-IMPACT)), as part of an institutional clinical cancer genomics initiative (16, 17). Separate IRB approvals were obtained at contributing institutions. Furthermore, tumors identified using fluorescence *in situ* hybridization studies were contributed from the consultation files of one of the authors (PA). In addition to 6 previously reported cases from The Cancer Genome Atlas, 12 renal tumors with 6p21.1 (*TFEB*) amplifications and 19 t(6;11) tumors were analyzed in this study (Figure 1). Specifically 9 (of 12) new cases of 6p21.1 (*TFEB*) amplification and 18 (of 19) cases with t(6;11) have not been previously reported in the literature (2, 18).

Immunohistochemistry and Fluorescence in Situ Hybridization

Immunohistochemistry for TFEB was performed using an automated staining platform (Bond-III, Leica Biosystems, Buffalo Grove, IL). A mouse monoclonal TFEB antibody was used as a primary reagent (clone: C-6, Santa Cruz Biotechnology, Dallas, TX) at a concentration of 0.2μg/ml. A polymeric secondary kit (Refine, Leica) was used for the detection of the primary antibody. Fluorescence in situ hybridization was performed as previously described using probes that cover and flank the *TFEB* gene on 6p21.1 (2, 18, 19). Nuclei with incomplete signals were omitted from the score and the threshold for rearrangements and amplifications included >20% split signals and >10:1 ratio of *TFEB* signal to reference, respectively.

Next Generation Sequencing-Based Copy Number Assessment: 6p21.1 (*TFEB*) Amplifications

Details of the MSK-IMPACT assay have been previously reported (16, 17). The MSK-IMPACT assay involves hybridization capture-based library preparation followed by deep sequencing of select non-coding regions and 6,614 protein-coding exons of 468 genes. Genome-wide copy number assessment is facilitated by homogenous distribution of single nucleotide polymorphism tiling probes across the genome. Based on previously reported criteria, gains were defined as a fold change ≥1.5 and <2.0, while amplifications were defined as a fold change ≥ 2.0 (20–22).

Digital Droplet PCR for Assessment of *TFEB* Gene Expression Status

RNA extraction was performed as previously described (23). Specifically, RNA was extracted from a minimum of three, 5-micron thick, sections of formalin fixed paraffin embedded tissue following review of the corresponding H&E stained slide by a single pathologist (SG) and manual macrodissection of areas of interest. Specific steps included the addition of 10 μl of mineral oil to each slide prior to macrodissection and the further addition of 800 μl of mineral oil for deparaffinization and RNA extraction using the RNeasy FFPE Kit and protocol (Qiagen). RNA quantification was performed using the Qubit Broad Range RNA Assay Kit (Life Tech.) and 2ng of template was used in subsequent reactions. The reaction mixtures for downstream processing included the One-Step RT-ddPCR Advanced Kit (Bio-Rad, CA) and PrimePCR- ddPCR- Expression Probe Assay for (human) *TFEB* (Bio-Rad, CA; Chromosome Location: 6:41655765–41658411; RefSeq: NC_000006.11;

Amplicon Length: 64). The QX200- Droplet Reader and QuantaSoft- Software (Bio-Rad, CA) were used to identify droplets containing amplification products using the FAM channel. *TFEB* gene expression was normalized to the expression of a corresponding housekeeping gene (*B2M*). All samples were tested in duplicate and samples were considered failures if a low number of total droplets (<10,000) was identified. Negative (no template) controls included water (n=4), while low positive controls included previously characterized cell free RNA samples (n=4). Non *TFEB*-altered controls (n=18) included non-neoplastic renal parenchyma (n=13) and renal tumors with no *TFEB* alterations detected on comprehensive molecular profiling using MSK-IMPACT (oncocytoma, n=2; clear cell renal cell carcinoma, n=3). A cutoff of 20% (*TFEB*: *B2M*) was selected retrospectively to distinguish tumors with *TFEB* alterations compared to those without *TFEB* alterations as this level of expression had a specificity of 100% in distinguishing these tumor types.

In a single case, t(6;11) was confirmed using anchored multiplex technology for fusion detection (Archer- FusionPlex-), as previously described (23).

Literature Review and Data Extraction from The Cancer Genome Atlas Datasets

The publicly available cBioPortal.32e34 platform was used to analyze data from The Cancer Genome Atlas and other public datasets (24). Six renal tumors with 6p21.1 (*TFEB*) amplifications were identified from previously reported The Cancer Genome Atlas datasets (2, 8, 14, 15).

Statistical Analysis

Continuous variables were evaluated with frequency counts and percentages. Tests used for the assessment of statistical significance were two-sided and $p<0.05$ was considered statistically significant.

Results

Next Generation Sequencing Results

All 5 renal tumors with 6p21.1 amplifications identified using MSK-IMPACT showed amplification of *CCND3* and/or *VEGFA* at this locus. The results of molecular profiling for 7 cases (5 *TFEB* amplification and 2 *TFEB* rearrangement) have been listed in Table1.

Clinical Features: *TFEB* rearranged and 6p21.1 (*TFEB*) Amplified Renal Tumors

Clinical features of patients diagnosed with renal tumors harboring *TFEB* alterations have been listed in Table 2 and summarized in Table 3. No significant gender predilection was identified. Of note, most of the tumors occurred in adults with only 5 (of 37, 14%) being diagnosed in individuals under the age of 25. Tumors with 6p21.1 (*TFEB*) amplifications, when compared to those with *TFEB* rearrangements, tended to be larger (mean size: 9.2cm vs 6.3cm; $p=0.04$). In addition, amongst a total of 15 cases where clinical follow-up was available, 6p21.1 (*TFEB*) amplified tumors had a higher incidence of documented regional or distant metastasis (88% vs 29%; $p=0.04$).

VEGFA amplifications have been reported to be present in renal tumors with 6p21.1 amplifications and therapy with anti-VEGF agents was documented for 2 patients with a 6p21.1 amplification and for 1 patient with a *TFEB* amplification in the background of a *TFEB* rearrangement, in our study (9, 11, 12). The first patient with a 6p21.1 amplification was a 61-year-old male who was diagnosed with a 13cm pT2b renal cell carcinoma and subsequently developed radiographic evidence of lung metastasis at 18 months of follow up. He was initially managed with bevacizumab and everolimus, and subsequently treated with other therapeutic agents (sunitinib, sorafenib, temsirolimus and nivolumab). Disease progression involved radiographic evidence of metastatic disease involving the lungs, mediastinal and hilar lymph nodes, liver and soft tissue. He eventually died of disease related complications at 55 months of follow up post-nephrectomy. The second patient with a 6p21.1 amplification was a 58-year-old male with a pT3b tumor with widely metastatic disease including extensive retroperitoneal lymphadenopathy and multiple hepatic metastasis. He was initially treated with pazopanib, followed by cabozantinib (VEGF inhibitor) and had stable disease for approximately 8 months. He eventually developed progressive disease and died of disease related complications at 1 year of follow up, post-initiation of therapy with pazopanib. The third patient with a *TFEB* amplification, in the background of a *COL21A1-TFEB* rearrangement, was a 64-year-old male with a pT3a tumor. This patient developed mediastinal lymphadenopathy at approximately 9 months of follow up. Initial management was with sunitinib followed by temsirolimus (tyrosine kinase inhibitor). Further disease progression involved osseous metastases and subsequently pulmonary metastasis. Subsequent management included immunotherapeutic agents such as nivolumab (immune checkpoint inhibitor). This patient is currently alive with stable disease at 187 days of follow up.

As these three cases represent limited reports of VEGF-directed therapy in patients with renal tumors that harbor *TFEB* alterations, no definitive conclusions could be drawn regarding therapeutic efficacy.

Histopathologic Features: *TFEB* rearranged and 6p21.1 (*TFEB*) Amplified Renal Tumors

Histologic features of patients diagnosed with renal tumors harboring *TFEB* alterations have been listed in Table 4 and summarized in Table 5. Representative images of these tumors have been depicted in Figures 2 and 3. These tumors were evaluated for features such as classic biphasic morphology which is characterized by tumor cells with clear to reticulated cytoplasm arranged in nests, alveoli or acini. Within these structures were smaller cells surrounding basement membrane-like material. Most of these cases showed immunohistochemical evidence of either cathepsin K, melan A or HMB45 expression (25 of 26, 96%) and tubulopapillary architectural patterns were seen in a third of these cases (12 of 36, 33.3%).

Cytologic features that helped in the separation of 6p21.1 (*TFEB*) amplified and *TFEB*-rearranged tumors included the presence of prominent cytoplasmic eosinophilia in the former (85.7% vs 27.3%; p=0.0016). Interestingly, while cytoplasmic eosinophilia was often seen in 6p21.1 amplified tumors, clear cytoplasm was frequently seen in *TFEB*-rearranged tumors (72.7% vs 14.3%; p=0.0016) (Figure 4). Classic biphasic morphology was not seen

in any 6p21.1 (*TFEB*) amplified renal tumor (0/14, 0%) and was seen in almost half of all cases with *TFEB* rearrangements (9 of 22, 41%; p=0.006). Therefore, when biphasic features are present, they are helpful in morphologically separating these two entities. Other features that did not reveal any statistically significant differences included papillary, tubulopapillary, solid, nested and acinar architectural patterns. Tumors with tubulopapillary, solid and alveolar/acinar architectural patterns have been illustrated in Figure 4. The presence of pigment and calcifications were documented in a limited number of cases. Similarly, features associated with adverse outcomes in renal tumors such as coagulative tumor necrosis, rhabdoid and sarcomatoid transformation were seen in occasional cases with both 6p21.1 amplifications and *TFEB* rearrangements. Interestingly, all 6p21.1 amplified tumors were at least WHO/ISUP grade3 or higher (14 of 14 cases, 100%) when compared to *TFEB*-rearranged tumors (9 of 22, 41%; p=0.0003).

TFEB Gene Expression: *TFEB* rearranged and 6p21.1 (*TFEB*) Amplified Renal Tumors

The results of *TFEB* gene expression profiling using digital PCR was correlated with immunohistochemistry for TFEB protein. Non-neoplastic renal parenchyma revealed a low-level of *TFEB* gene expression and this correlated with the nuclear expression of TFEB in a subset of renal tubules in all cases that were tested (Figure 5a–d). Preliminary results suggest that TFEB protein expression is restricted to distal tubules and future studies are needed to confirm this observation. Interestingly, the background level of *TFEB* gene expression in renal tumors that lacked *TFEB* alterations trended lower compared to non-neoplastic renal parenchyma (mean: 3.9% vs 8.2%; Figure 5e). *TFEB* gene expression in renal tumors with (n=28) and without (n=5) known *TFEB* alterations was assessed relative to *TFEB* gene expression in non-neoplastic renal parenchyma. In contrast to tumors that lacked *TFEB* amplifications/rearrangements, most tumors with *TFEB* alterations showed higher gene expression compared to non-neoplastic renal parenchyma (Figure 5d, f; p=0.0005).

Unlike immunohistochemistry, digital PCR to assess *TFEB* gene expression did not account for tumor heterogeneity. Two cases have been highlighted where the macrodissected tumor included either a sarcomatoid component (Figure 6a–d) or a second population of intra-luminal smaller viable cells (Figure 6e–f) that completely lacked nuclear TFEB protein expression by immunohistochemistry. Of note, the case with intra-luminal smaller cells did not show classic biphasic morphology characterized by smaller cells surrounding basement membrane-like material (Figure 6e–f). These elements likely contributed to a lower estimate for overall *TFEB* gene expression for both tumors.

As expected, renal tumors with known *TFEB* alterations had significantly higher *TFEB* gene expression when compared to appropriate controls (Figure 7a). A cutoff of 20% *TFEB* gene expression had a sensitivity of 78.6% (22 of 28 cases) for detecting these cases and a specificity of 100% for discriminating these from non *TFEB*-altered tumors (n=18) (Figure 7b). Of note, cases with *TFEB* amplification tended to have lower expression of this gene compared to cases with rearrangements (mean: 51.2% vs 224.7%, p=0.06; Figure 7c and Table 5).

Amongst tumors with known *TFEB* alterations, correlation of morphology with *TFEB* gene expression revealed that those with classic biphasic histologic features had significantly

higher *TFEB* gene expression (mean: 401.7% vs 58.7%, p=0.00004; Figure 7d). A case with a known *COL21A1-TFEB* rearrangement occurring in the background of a 6p21.1 (*TFEB*) amplification (TCGA-BQ-7048) is highlighted in support of this observation (Figure 8a–f) (15). Two morphologically distinct areas from the same tumor were separately macrodissected and profiled for *TFEB* gene expression status. Areas with clear cell change showed lower gene and protein expression (Figure 8a–b) compared to areas that had features reminiscent of an oncocytoma (Figure 8c–d) adjacent to tumor with biphasic morphologic features (Figure 8e–f).

Discussion

TFEB-overexpressing renal tumors were initially described in pediatric patient populations and are being increasingly identified in adult patients. This observation is supported by the results of our study (1). Amongst *TFEB*-overexpressing tumors, those harboring 6p21.1 (*TFEB*) amplifications were only recently described and emerging data suggests that these tumors have a more aggressive clinical course compared to *TFEB*-rearranged tumors (11).

In this regard, the English language literature was reviewed to determine the relative incidence of renal tumors with 6p21.1 (*TFEB*) amplifications and *TFEB* rearrangements, as well as documented cases of regional and distant metastatic disease for both tumor types (Table 6). This information was combined with results of the current study. For tumors harboring *TFEB* rearrangements we identified at least 13 cases with regional or distant metastasis (13, 18, 19, 25–31). These reports of aggressive disease were identified from approximately 106 cases (12%) reported between 1996 to 2019 and many of the reported cases had limited long-term follow up (1, 3–7, 10, 13–15, 18, 19, 25–50). In contrast, within a much shorter span of time (2014–2019) at least 25 6p21.1 (*TFEB*) amplified renal tumors with regional or distant metastasis have been reported (2, 6, 8–12, 14, 15, 31, 51). These reports were identified amongst 57 cases (44%) and a limited long-term follow up was documented for many of these cases as well (2, 6–12, 14, 15, 31, 47, 48, 51–53). The results of our study support this trend as well. Furthermore, at least 8 of 16 (50%) reported cases of renal tumors with lower level gains (defined as <10:1 ratio of *TFEB* signal to reference) at the 6p21.1 locus exhibited aggressive behavior (9, 11). Therefore, as recognition of this entity grows, future studies may be needed to refine diagnostic definitions, taking into consideration both tumor biology and outcomes.

Broad molecular characterization of these tumors in prior studies had reported chromosome 3p loss/*VHL* alterations in a total of 7 such cases and two cases in our study showed 3p loss/*VHL* alteration (The Cancer Genome Atlas/Williamson et al, n=5; Mendel et al, n=2; MSK-IMPACT/current study, n=2; Table1) (7, 8, 12, 15). Overall, no recurrent alteration other than amplified oncogenes at 6p21.1 were identified in 5 such cases. It could therefore be hypothesized that the primary driver alterations in these tumors include *TFEB* and oncogenes present at the 6p21.1 locus (8, 12, 14, 15). *VEGFA* and *CCND3* at the 6p21.1 locus are two candidate genes which could promote aggressive biologic behavior in these tumors and a few studies have documented alterations of the former in 6p21.1 amplified tumors (7, 9, 11, 12). However, the level of *TFEB* overexpression in these tumors was an

unanswered question. Herein we have correlated *TFEB* gene expression with various clinicopathologic features to better understand the biology of these tumors.

Our current series of 37 cases (including 5 cases from The Cancer Genome Atlas dataset) was used to evaluate for histopathologic features that might be helpful in diagnosing these tumors. Our study suggests that renal tumors with alterations of the *TFEB* gene show significant morphologic heterogeneity. These results suggest that some morphologic features may be helpful in screening renal tumors for further characterization with ancillary immunohistochemical and molecular techniques, to establish a more precise diagnosis. Specifically, our results suggest that 6p21.1 (*TFEB*) amplified tumors exhibit tubulopapillary architecture and prominent cytoplasmic eosinophilia in close to half of these cases. Features helpful in the separation of *TFEB* amplified and rearranged tumors include cytoplasmic eosinophilia and high WHO/ISUP grade (≥ grade 3) in the former. Interestingly, classic biphasic morphology characterized by smaller cells surrounding basement membrane-like material was only seen in *TFEB*-rearranged tumors (41% of cases) and was not identified in any case with isolated 6p21.1 amplifications. This trend is consistent with what has been reported in the literature for (non-TCGA) 6p21.1 amplified cases (Argani et al: 2/8 cases; Williamson et al: 0/3 cases; Gupta et al: 3/11 cases; Skala et al: 0/6 cases; Mendel et al: 0/3 cases; Calio et al: 0/3 cases) (2, 8–12). Furthermore, tumors that exhibited classic biphasic features tended to have on average a 6.8-fold higher level of *TFEB* gene expression.

It is, however, important to note that some cases have a *TFEB*-rearrangement in the background of a 6p21.1 amplification and it may be challenging to identify rearrangement events in such cases using break-apart fluorescent in situ hybridization probes (7, 14, 15). Herein, we highlight one such case with a *COL21A1-TFEB* rearrangement that exhibited classic biphasic features (15). Finally, immunohistochemistry for either cathepsin K/ melan A or HMB45 was an effective screen and was able to identify >95% of cases for confirmatory testing.

At a cutoff of 20% *TFEB*: *B2M* expression, the sensitivity of the digital PCR assay in discriminating *TFEB* mRNA over-expressing tumors from non-*TFEB* overexpressing tumors was 78.6%, while maintaining a specificity of 100%. The lower sensitivity, at lower levels of *TFEB* gene expression, can in part be attributed to the inclusion of elements of non-neoplastic renal parenchyma in macrodissected tissue for downstream analysis. Other confounding variables, determined by correlations with corresponding immunohistochemistry, include tumor heterogeneity and *TFEB* gene expression in lymphoid infiltrates.

Important observations included a trend of lower *TFEB* gene expression in 6p21.1 (*TFEB*) amplified tumors (n=9, mean expression: 51.2%) compared to *TFEB*-rearranged tumors (n=19, mean expression: 224.7%, p=0.06). This was correlated with over 40% of the 6p21.1 amplified tumors showing *TFEB* gene expression under the 20% cutoff and with at least 2 cases lacking expression of screening markers (cathepsin K, melan A, HMB45, n=1; TFEB, n=1) by immunohistochemistry. These results suggest that the aggressive behavior of 6p21.1 (*TFEB*) amplified tumors may not be linked to higher levels of *TFEB* gene expression in these tumors. Our study therefore adds to the scientific literature by helping to establish a

rationale for identifying other pathogenic alterations that may drive aggressive behavior in 6p21.1 (*TFEB*) amplified tumors.

In summary, our model for differing pathogenic mechanisms in 6p21.1 (*TFEB*) amplified compared to *TFEB*-rearranged tumors is shown in Figure 9. Our data suggests that *TFEB*-amplified tumors have lower (*TFEB*) gene expression compared to *TFEB*-rearranged tumors. This, however, does not explain the more aggressive biologic behavior of these tumors, which might be better explained by other alterations including the amplification of additional oncogenes at the 6p21.1 locus. Finally, classic biphasic morphology appears to be primarily seen in *TFEB*-rearranged tumors and is correlated with significantly higher levels of *TFEB* gene expression.

Acknowledgement

The authors would like to thank Jessica M. Menzel, Jennifer Posada and Christine Moon for administrative assistance.

Disclosures: The authors of this article have no relevant financial relationships with commercial interests to disclose. This study was supported in part through NIH/NCI Cancer Center Support grant P30CA008748.

References

1. Argani P, Hawkins A, Griffin CA, et al. A distinctive pediatric renal neoplasm characterized by epithelioid morphology, basement membrane production, focal HMB45 immunoreactivity, and t(6;11)(p21.1;q12) chromosome translocation. Am J Pathol. 2001;158:2089–2096. [PubMed: 11395386]
2. Argani P, Reuter VE, Zhang L, et al. TFEB-amplified renal cell carcinomas: an aggressive molecular subset demonstrating variable melanocytic marker expression and morphologic heterogeneity. Am J Surg Pathol. 2016;40:1484–1495. [PubMed: 27565001]
3. Dijkhuizen T, Berg EV, Störkel S, et al. Two cases of renal cell carcinoma, clear cell type, revealing a t(6;11)(p21;q13). Cancer Genetics; 1996:141.
4. van Asseldonk M, Schepens M, de Bruijn D, et al. Construction of a 350-kb sequence-ready 11q13 cosmid contig encompassing the markers D11S4933 and D11S546: mapping of 11 genes and 3 tumor-associated translocation breakpoints. Genomics. 2000;66:35–42. [PubMed: 10843802]
5. Kuiper RP, Schepens M, Thijssen J, et al. Upregulation of the transcription factor TFEB in t(6;11)(p21;q13)-positive renal cell carcinomas due to promoter substitution. Hum Mol Genet. 2003;12:1661–1669. [PubMed: 12837690]
6. Peckova K, Vanecek T, Martinek P, et al. Aggressive and nonaggressive translocation t(6;11) renal cell carcinoma: comparative study of 6 cases and review of the literature. Ann Diagn Pathol. 2014;18:351–357. [PubMed: 25438924]
7. Durinck S, Stawiski EW, Pavia-Jimenez A, et al. Spectrum of diverse genomic alterations define non-clear cell renal carcinoma subtypes. Nat Genet. 2015;47:13–21. [PubMed: 25401301]
8. Williamson SR, Grignon DJ, Cheng L, et al. Renal cell carcinoma with chromosome 6p amplification including the TFEB gene: a novel mechanism of tumor pathogenesis? Am J Surg Pathol. 2017;41:287–298. [PubMed: 28009604]
9. Gupta S, Johnson SH, Vasmatzis G, et al. TFEB-VEGFA (6p21.1) co-amplified renal cell carcinoma: a distinct entity with potential implications for clinical management. Mod Pathol. 2017;30:998–1012. [PubMed: 28338654]
10. Skala SL, Xiao H, Udager AM, et al. Detection of 6 TFEB-amplified renal cell carcinomas and 25 renal cell carcinomas with MITF translocations: systematic morphologic analysis of 85 cases evaluated by clinical TFE3 and TFEB FISH assays. Mod Pathol. 2018;31:179–197. [PubMed: 28840857]

11. Calio A, Brunelli M, Segala D, et al. VEGFA amplification/increased gene copy number and VEGFA mRNA expression in renal cell carcinoma with TFEB gene alterations. Mod Pathol. 2018.
12. Mendel L, Ambrosetti D, Bodokh Y, et al. Comprehensive study of three novel cases of TFEB-amplified renal cell carcinoma and review of the literature: Evidence for a specific entity with poor outcome. Genes Chromosomes Cancer. 2018;57:99–113. [PubMed: 29127730]
13. Calio A, Brunelli M, Segala D, et al. t(6;11) renal cell carcinoma: a study of seven cases including two with aggressive behavior, and utility of CD68 (PG-M1) in the differential diagnosis with pure epithelioid PEComa/epithelioid angiomyolipoma. Mod Pathol. 2018;31:474–487. [PubMed: 29052596]
14. Malouf GG, Su X, Yao H, et al. Next-generation sequencing of translocation renal cell carcinoma reveals novel RNA splicing partners and frequent mutations of chromatin-remodeling genes. Clin Cancer Res. 2014;20:4129–4140. [PubMed: 24899691]
15. Cancer Genome Atlas Research N, Linehan WM, Spellman PT, et al. Comprehensive molecular characterization of papillary renal-cell carcinoma. N Engl J Med. 2016;374:135–145. [PubMed: 26536169]
16. Cheng DT, Mitchell TN, Zehir A, et al. Memorial Sloan Kettering-Integrated Mutation Profiling of Actionable Cancer Targets (MSK-IMPACT): a hybridization capture-based next-generation sequencing clinical assay for solid tumor molecular oncology. J Mol Diagn. 2015;17:251–264. [PubMed: 25801821]
17. Zehir A, Benayed R, Shah RH, et al. Mutational landscape of metastatic cancer revealed from prospective clinical sequencing of 10,000 patients. Nat Med. 2017;23:703–713. [PubMed: 28481359]
18. Smith NE, Illei PB, Allaf M, et al. t(6;11) renal cell carcinoma (RCC): expanded immunohistochemical profile emphasizing novel RCC markers and report of 10 new genetically confirmed cases. Am J Surg Pathol. 2014;38:604–614. [PubMed: 24618616]
19. Argani P, Yonescu R, Morsberger L, et al. Molecular confirmation of t(6;11)(p21;q12) renal cell carcinoma in archival paraffin-embedded material using a break-apart TFEB FISH assay expands its clinicopathologic spectrum. Am J Surg Pathol. 2012;36:1516–1526. [PubMed: 22892601]
20. Ross DS, Zehir A, Cheng DT, et al. Next-generation assessment of Human Epidermal Growth Factor Receptor 2 (ERBB2) amplification status: clinical validation in the context of a hybrid capture-based, comprehensive solid tumor genomic profiling assay. J Mol Diagn. 2017;19:244–254. [PubMed: 28027945]
21. Gupta S, Vanderbilt CM, Cotzia P, et al. JAK2, PD-L1, and PD-L2 (9p24.1) amplification in metastatic mucosal and cutaneous melanomas with durable response to immunotherapy. Hum Pathol. 2018.
22. Gupta S, Vanderbilt CM, Cotzia P, et al. Next-generation sequencing-based assessment of JAK2, PD-L1, and PD-L2 copy number alterations at 9p24.1 in breast cancer: potential implications for clinical management. J Mol Diagn. 2018.
23. Zhu G, Benayed R, Ho C, et al. Diagnosis of known sarcoma fusions and novel fusion partners by targeted RNA sequencing with identification of a recurrent ACTB-FOSB fusion in pseudomyogenic hemangioendothelioma. Mod Pathol. 2018.
24. Gao J, Aksoy BA, Dogrusoz U, et al. Integrative analysis of complex cancer genomics and clinical profiles using the cBioPortal. Sci Signal. 2013;6:pl1. [PubMed: 23550210]
25. Pecciarini L, Cangi MG, Lo Cunsolo C, et al. Characterization of t(6;11)(p21;q12) in a renal-cell carcinoma of an adult patient. Genes Chromosomes Cancer. 2007;46:419–426. [PubMed: 17285572]
26. Camparo P, Vasiliu V, Molinie V, et al. Renal translocation carcinomas: clinicopathologic, immunohistochemical, and gene expression profiling analysis of 31 cases with a review of the literature. Am J Surg Pathol. 2008;32:656–670. [PubMed: 18344867]
27. Ishihara A, Yamashita Y, Takamori H, et al. Renal carcinoma with (6;11)(p21;q12) translocation: report of an adult case. Pathol Int. 2011;61:539–545. [PubMed: 21884304]
28. Inamura K, Fujiwara M, Togashi Y, et al. Diverse fusion patterns and heterogeneous clinicopathologic features of renal cell carcinoma with t(6;11) translocation. Am J Surg Pathol. 2012;36:35–42. [PubMed: 22173116]

29. Hora M, Urge T, Travnicek I, et al. MiT translocation renal cell carcinomas: two subgroups of tumours with translocations involving 6p21 [t (6; 11)] and Xp11.2 [t (X;1 or X or 17)]. Springerplus. 2014;3:245. [PubMed: 24877033]
30. Lilleby W, Vlatkovic L, Meza-Zepeda LA, et al. Translocational renal cell carcinoma (t(6;11)(p21;q12) with transcription factor EB (TFEB) amplification and an integrated precision approach: a case report. J Med Case Rep. 2015;9:281. [PubMed: 26654961]
31. Kojima F, Kuroda N, Matsuzaki I, et al. Aggressive TFEB-rearranged renal cell carcinoma mimicking chromophobe and clear cell renal cell carcinoma. Pathol Int. 2019.
32. Davis IJ, Hsi BL, Arroyo JD, et al. Cloning of an Alpha-TFEB fusion in renal tumors harboring the t(6;11)(p21;q13) chromosome translocation. Proc Natl Acad Sci U S A. 2003;100:6051–6056. [PubMed: 12719541]
33. Argani P, Lae M, Hutchinson B, et al. Renal carcinomas with the t(6;11)(p21;q12): clinicopathologic features and demonstration of the specific alpha-TFEB gene fusion by immunohistochemistry, RT-PCR, and DNA PCR. Am J Surg Pathol. 2005;29:230–240. [PubMed: 15644781]
34. Argani P, Lae M, Ballard ET, et al. Translocation carcinomas of the kidney after chemotherapy in childhood. J Clin Oncol. 2006;24:1529–1534. [PubMed: 16575003]
35. Hora M, Hes O, Urge T, et al. A distinctive translocation carcinoma of the kidney ["rosette-like forming," t(6;11), HMB45-positive renal tumor]. Int Urol Nephrol. 2009;41:553–557. [PubMed: 18998233]
36. Zhan HQ, Wang CF, Zhu XZ, et al. Renal cell carcinoma with t(6;11) translocation: a patient case with a novel Alpha-TFEB fusion point. J Clin Oncol. 2010;28:e709–713. [PubMed: 20823414]
37. Zhong M, De Angelo P, Osborne L, et al. Translocation renal cell carcinomas in adults: a single-institution experience. Am J Surg Pathol. 2012;36:654–662. [PubMed: 22446944]
38. Rao Q, Liu B, Cheng L, et al. Renal cell carcinomas with t(6;11)(p21;q12): A clinicopathologic study emphasizing unusual morphology, novel alpha-TFEB gene fusion point, immunobiomarkers, and ultrastructural features, as well as detection of the gene fusion by fluorescence in situ hybridization. Am J Surg Pathol. 2012;36:1327–1338. [PubMed: 22895266]
39. Rao Q, Zhang XM, Tu P, et al. Renal cell carcinomas with t(6;11)(p21;q12) presenting with tubulocystic renal cell carcinoma-like features. Int J Clin Exp Pathol. 2013;6:1452–1457. [PubMed: 23826432]
40. Matsuura K, Inoue T, Kai T, et al. Molecular analysis of a case of renal cell carcinoma with t(6;11)(p21;q12) reveals a link to a lysosome-like structure. Histopathology. 2014;64:306–309. [PubMed: 24117748]
41. Chaste D, Vian E, Verhoest G, et al. Translocation renal cell carcinoma t(6;11)(p21;q12) and sickle cell anemia: first report and review of the literature. Korean J Urol. 2014;55:145–147. [PubMed: 24578813]
42. Falzarano SM, McKenney JK, Montironi R, et al. Renal cell carcinoma occurring in patients with prior neuroblastoma: a heterogenous group of neoplasms. Am J Surg Pathol. 2016;40:989–997. [PubMed: 26975037]
43. Saleeb RM, Srigley JR, Sweet J, et al. Melanotic MiT family translocation neoplasms: expanding the clinical and molecular spectrum of this unique entity of tumors. Pathol Res Pract. 2017;213:1412–1418. [PubMed: 28969862]
44. Williamson SR, Eble JN, Palanisamy N. Sclerosing TFEB-rearrangement renal cell carcinoma: a recurring histologic pattern. Hum Pathol. 2017;62:175–179. [PubMed: 27864122]
45. Suarez-Vilela D, Izquierdo-Garcia F, Mendez-Alvarez JR, et al. Renal translocation carcinoma with expression of TFEB: presentation of a case with distinctive histological and immunohistochemical features. Int J Surg Pathol. 2011;19:506–509. [PubMed: 19687027]
46. Cajaiba MM, Dyer LM, Geller JI, et al. The classification of pediatric and young adult renal cell carcinomas registered on the children's oncology group (COG) protocol AREN03B2 after focused genetic testing. Cancer. 2018;124:3381–3389. [PubMed: 29905933]
47. Wyvekens N, Rechsteiner M, Fritz C, et al. Histological and molecular characterization of TFEB-rearranged renal cell carcinomas (In Press). Virchows Arch. 2019.

48. Martin EE, Mehra R, Jackson-Cook C, et al. Renal cell carcinoma with TFEB translocation versus unclassified renal cell carcinoma with TFEB amplification. 2017;22:305–312.

49. Kuroda N, Yorita K, Sasaki N, et al. Clinicopathological study of 5 cases of renal cell carcinoma with t(6;11)(p21;q12). Pol J Pathol. 2017;68:66–72. [PubMed: 28547982]

50. Petersson F, Vanecek T, Michal M, et al. A distinctive translocation carcinoma of the kidney; “rosette forming,” t(6;11), HMB45-positive renal tumor: a histomorphologic, immunohistochemical, ultrastructural, and molecular genetic study of 4 cases. Hum Pathol. 2012;43:726–736. [PubMed: 22051379]

51. Qu X, Tretiakova MS, Chen Y, et al. TFEB amplification renal cell carcinoma detected by chromosome genomic array testing: a case report for diagnosis of a novel entity. Journal of Clinical and Molecular Pathology. 2017;1:7 Available from: iMedPub, Hyderabad, India. Accessed March12, 2019.

52. Andeen NK, Qu X, Antic T, et al. Clinical utility of chromosome genomic array testing for unclassified and advanced-stage renal cell carcinomas. Arch Pathol Lab Med. 2018.

53. Mayoral Guisado C, Gómez Durán Á, Agustín Benítez López D, et al. [TFEB-amplified renal cell carcinoma. A case report and review of the literature]. Rev Esp Patol. 2018;51:248–252. [PubMed: 30269777]

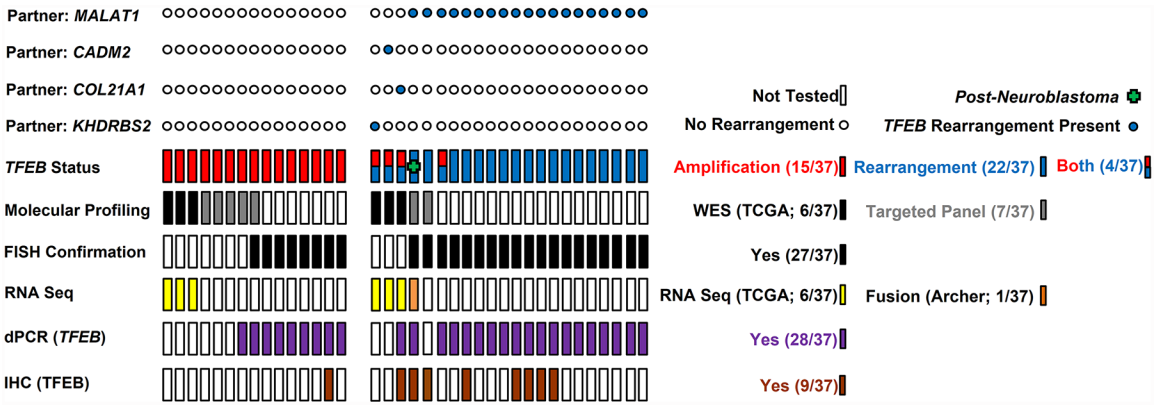

Figure 1: Methods.

Graphical representation of different methodologies used to interrogate renal tumors with 6p21.1 (*TFEB*) amplifications and rearrangements, including molecular profiling (whole exome sequencing, targeted panels), fluorescent in situ hybridization (FISH), RNA sequencing (RNASeq, anchored multiplex technology), digital PCR (dPCR) and immunohistochemistry (IHC). Fusion partners for *TFEB* rearranged genes have been indicated. TCGA: The Cancer Genome Atlas.

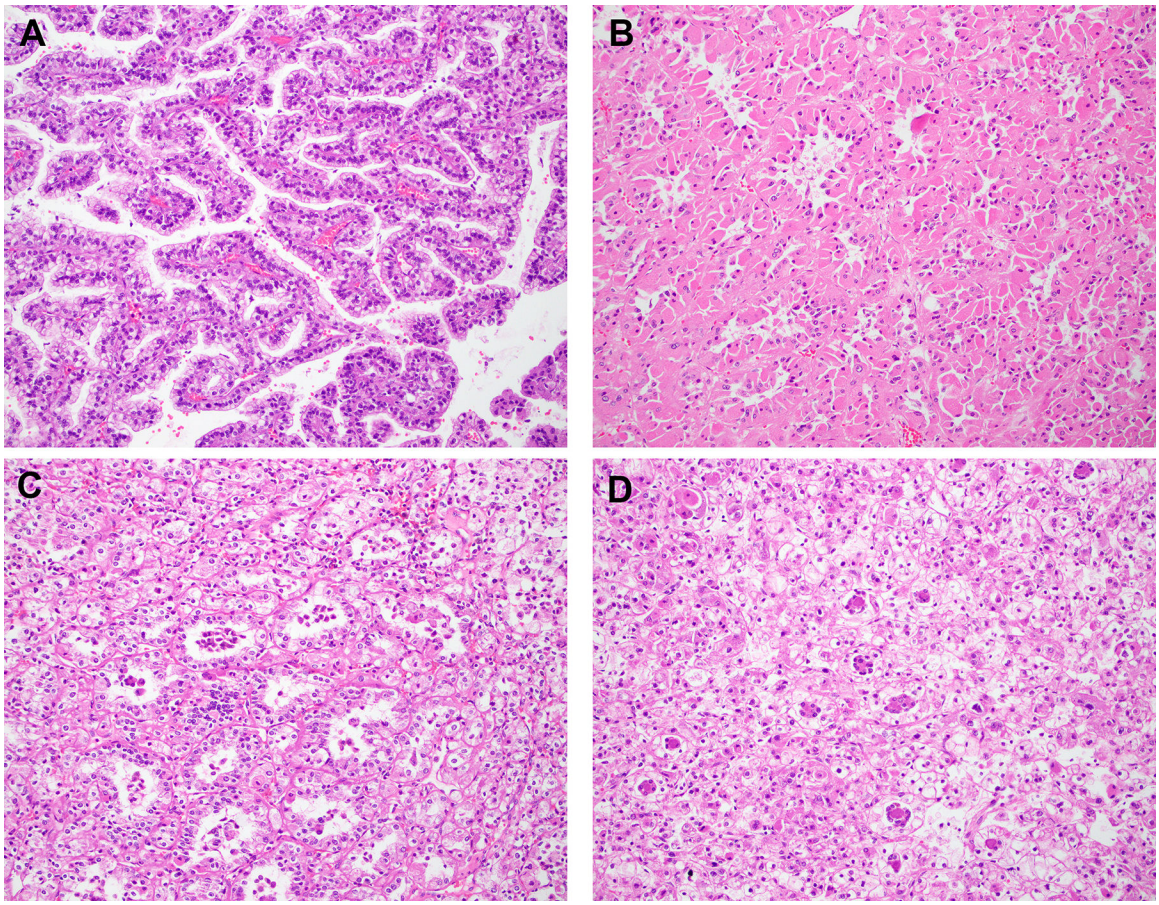

Figure 2: Histopathology.

Representative H&E stained images of *TFEB*-rearranged renal tumors and corresponding digital PCR quantification for *TFEB* are depicted ((a) papillary, *TFEB/B2M*=26%; (b) tubulopapillary with prominent cytoplasmic eosinophilia, *TFEB/B2M*=46%; (c, d) classic biphasic; × 200 magnification, c: *TFEB/B2M*=217% and d: *TFEB/B2M*=890%).

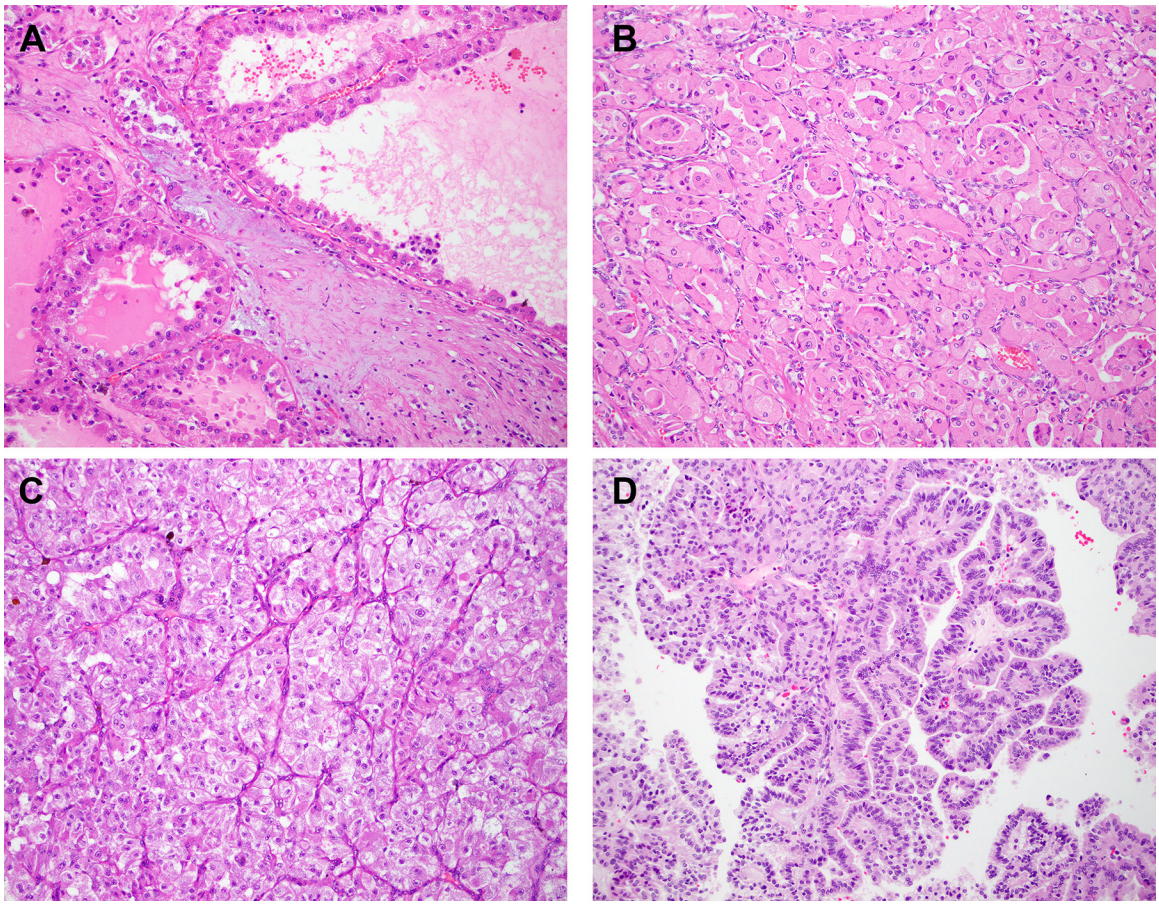

Figure 3: Histopathology.

Representative H&E stained images of 6p21.1 (*TFEB*)-amplified renal tumors and corresponding digital PCR quantification for *TFEB* are depicted ((a) cystic, *TFEB/B2M*=10.5%; (b) tubulopapillary, *TFEB/B2M*=66.5%; (c) alveolar/acinar, *TFEB/B2M*=85.4%; (d) papillary, × 200 magnification, digital PCR not performed).

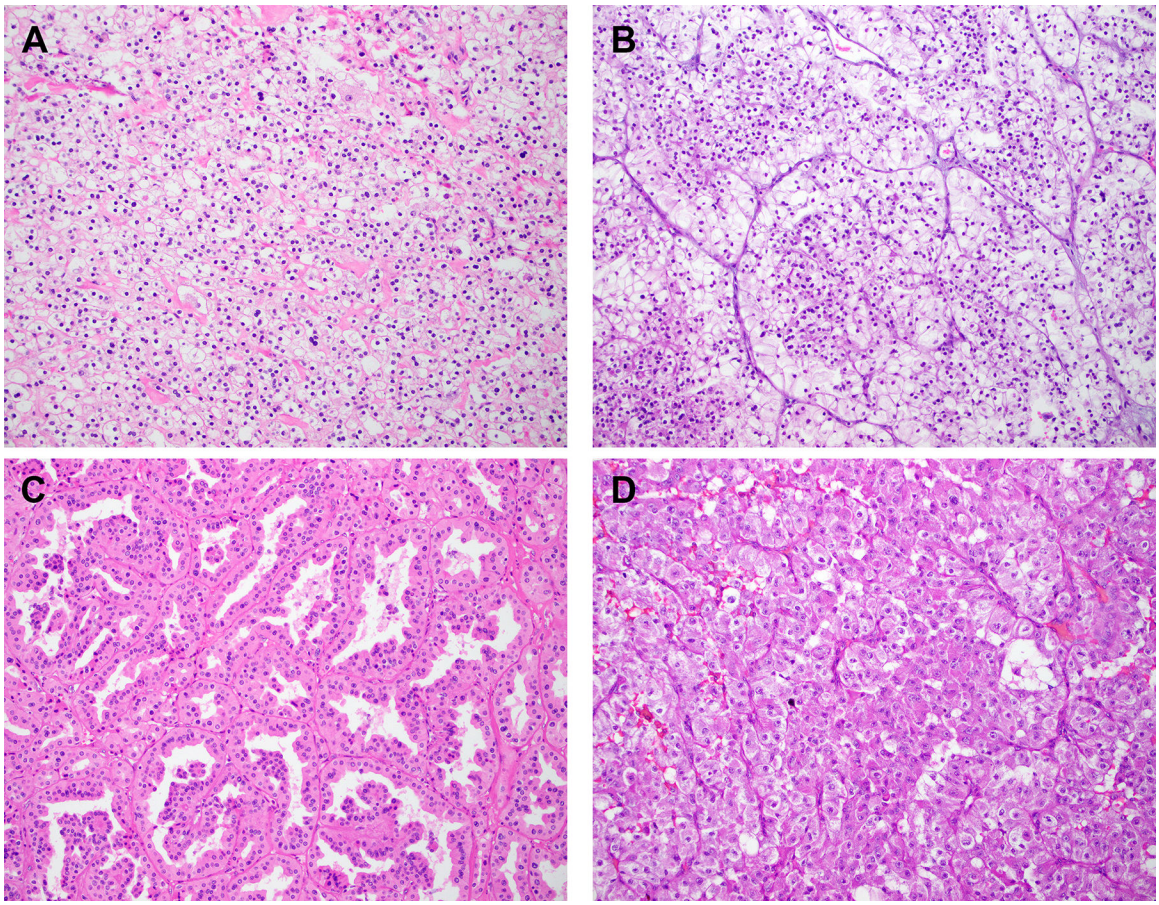

Figure 4: Histopathology.

Representative H&E stained images of *TFEB*-rearranged renal tumors with clear cytoplasm ((a) solid architecture; (b) alveolar/acinar architecture; × 200 magnification) and 6p21.1 (*TFEB*) amplified renal tumors with cytoplasmic eosinophilia ((c) tubulopapillary architecture; (d) solid to alveolar/acinar architecture; × 200 magnification) have been depicted.

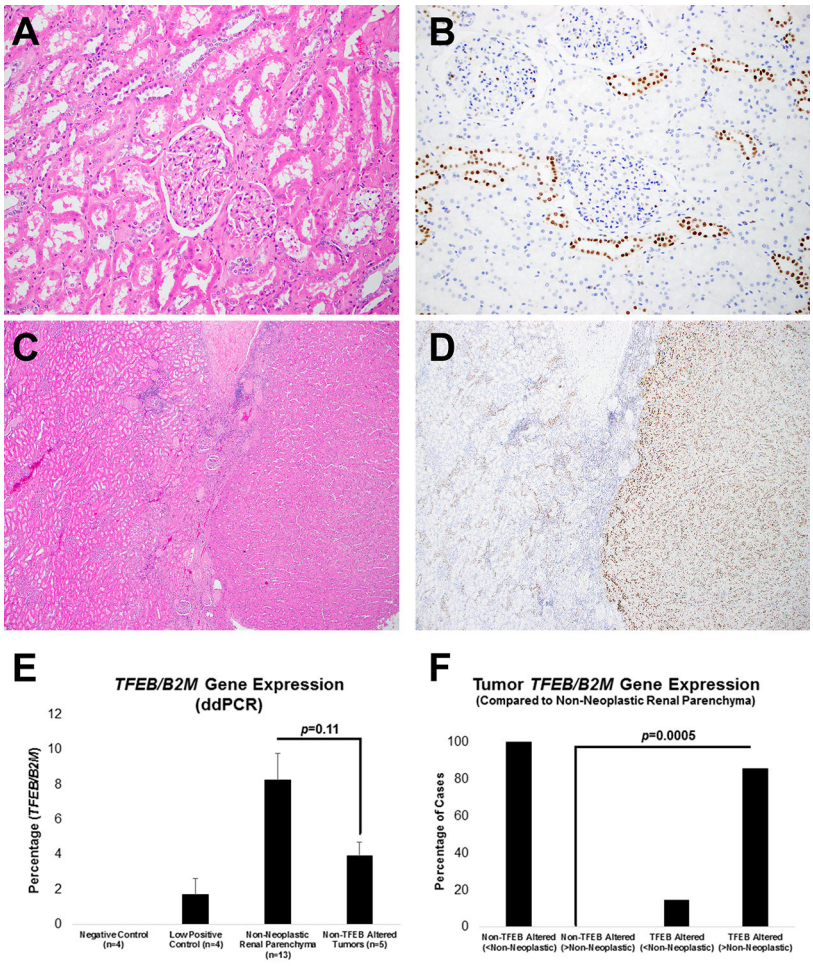

Figure 5: Histopathology, Immunohistochemistry and Digital Droplet PCR (Non-Neoplastic Renal Tissue).

Representative H&E stained images of non-neoplastic renal parenchyma adjacent to tumors with *TFEB* alterations is depicted ((a) × 200 magnification, 7.5% *TFEB* gene expression by digital PCR; (c) × 40 magnification, 3.7% *TFEB* gene expression by digital PCR). Corresponding immunostaining for TFEB shows scattered distal tubules with nuclear expression ((b) × 200 magnification; (d) × 40 magnification, with approximately >12-fold *TFEB* gene expression by digital PCR in the adjacent *TFEB*-rearranged renal tumor). Non-neoplastic renal parenchyma (n=13), when compared to non *TFEB*-altered renal tumors (n=5), showed a trend towards higher *TFEB* gene expression ((e) digital PCR). *TFEB* gene expression (normalized to *B2M*) was measured using digital PCR in both renal tumor types (with or without *TFEB* alterations) and in non-neoplastic renal parenchyma. Tumors that lacked *TFEB* amplifications/rearrangements showed lower expression compared to non-neoplastic renal parenchyma (f). In contrast, most tumors with *TFEB* alterations showed higher expression compared to non-neoplastic renal parenchyma (f).

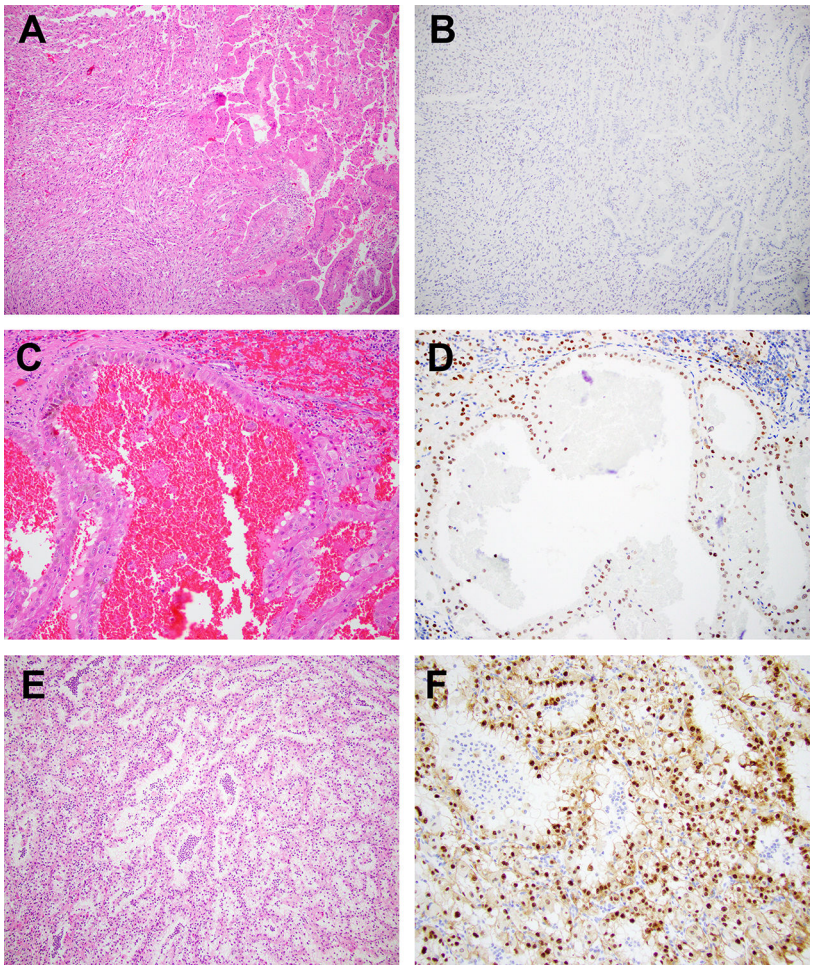

Figure 6: Histopathology and Immunohistochemistry (Tumor Heterogeneity).

Representative H&E stained images of a *TFEB*-rearranged renal tumor is depicted ((a) × 200 magnification, showing transition to sarcomatoid areas; (c) × 200 magnification, no sarcomatoid transformation). Corresponding immunostaining for TFEB shows absent expression in areas of sarcomatoid transformation (b) compared to nuclear expression in areas without sarcomatoid transformation (d). *TFEB* gene expression by digital PCR in both areas combined was 2.9%. Representative H&E stained image of a second *TFEB*-rearranged renal tumor ((e) × 40 magnification, 149% *TFEB* gene expression by digital PCR) shows a second population of intra-luminal, smaller viable cells that lack TFEB expression by immunohistochemistry (f).

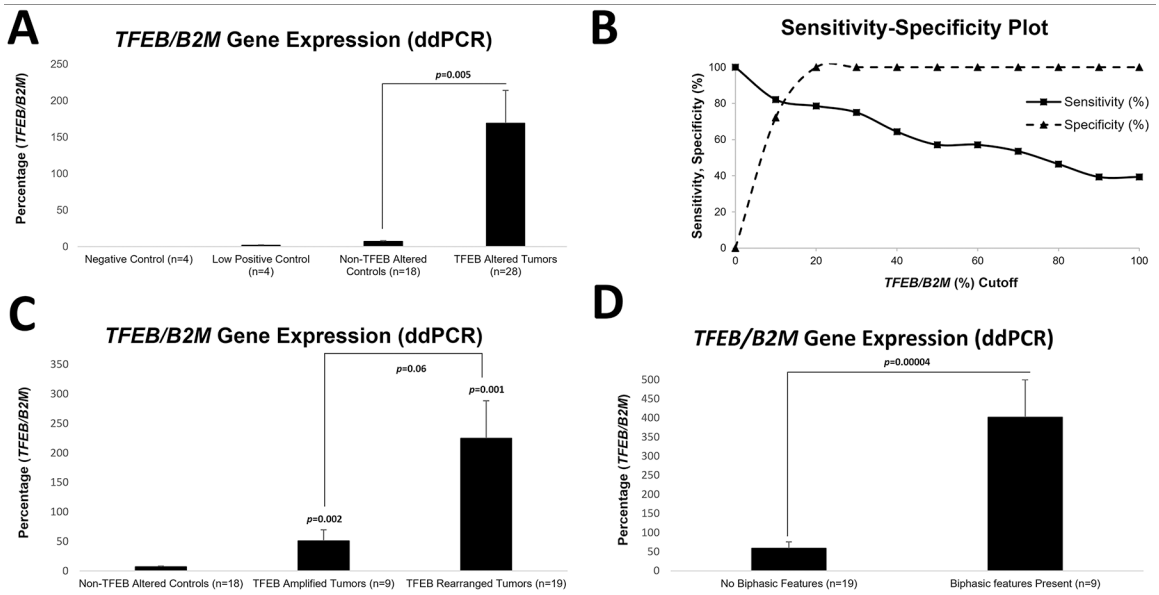

Figure 7: Digital Droplet PCR to Quantify *TFEB* Gene Expression.

Mean values of *TFEB* gene expression, comparing renal tumors with 6p21.1 (*TFEB*) amplification/*TFEB* rearrangement to non-*TFEB* altered controls is shown in (a). The relative sensitivity and specificity, for every 10% incremental increase in *TFEB* gene expression (normalized to *B2M*, digital PCR), for the detection of renal tumors with *TFEB* alterations is depicted (b). Comparisons of *TFEB* gene expression between renal tumors with 6p21.1 (*TFEB*) amplifications and *TFEB* rearrangements (c) and *TFEB*-altered renal tumors with or without biphasic morphologic features (d) is depicted.

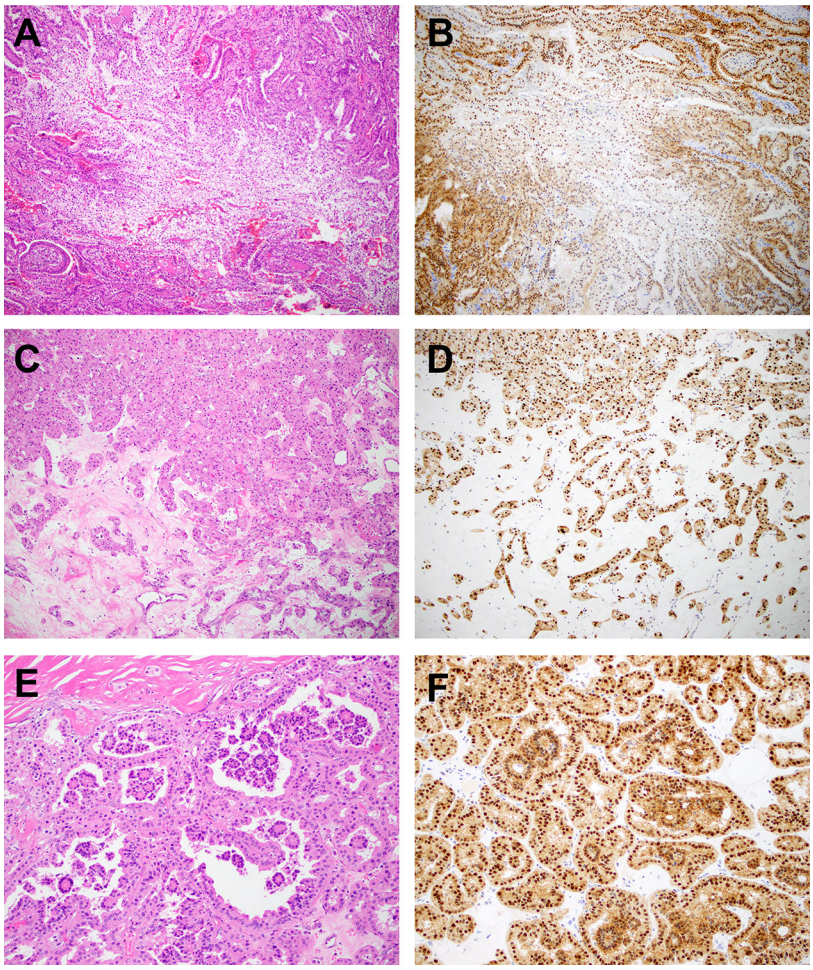

Figure 8: Histopathology and Immunohistochemistry (*TFEB* Rearranged (*COL21A1-TFEB*) and 6p21.1 (*TFEB*) Amplified Tumor).

Representative H&E and TFEB immunohistochemistry is shown for two morphologically distinct areas of a renal tumor with a *COL21A1-TFEB* rearrangement and associated 6p21.1 (*TFEB*) amplification which were separately macrodissected and profiled for *TFEB* gene expression status. An area of clear cell change is depicted ((a) × 100 magnification, (b) low/absent TFEB nuclear expression by immunohistochemistry, 72% *TFEB* gene expression by digital PCR). Other areas of the same tumor show features reminiscent of an oncocytoma ((c) × 100 magnification) and classic biphasic morphology that is characteristic of t(6;11) renal tumors ((e) × 100 magnification). These areas showed strong TFEB nuclear expression by immunohistochemistry (d, f) and higher (304%) *TFEB* gene expression by digital PCR.

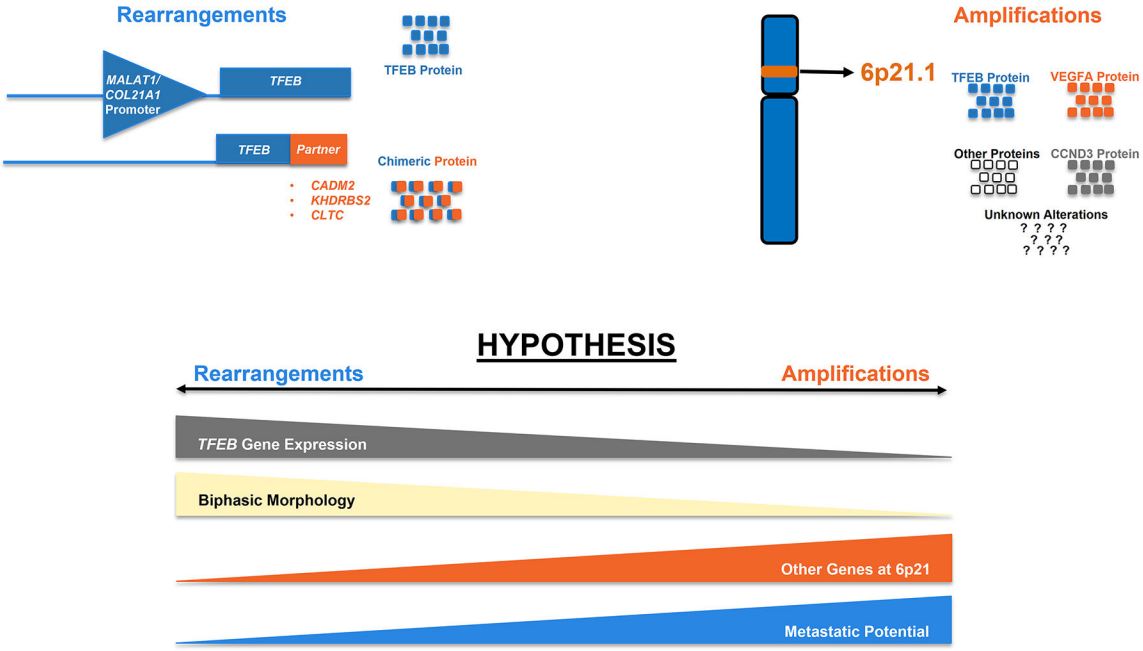

Figure 9: Schematic Representation: Correlation of *TFEB* Gene Expression Status with Tumor Biology.

A graphical representation of the hypothesized spectrum of *TFEB* gene expression, biphasic morphologic features, 6p21.1 gene expression correlated with metastatic potential in renal tumors with *TFEB* rearrangements compared to those with 6p21.1 (*TFEB*) amplifications is depicted.

Table1.

Molecular Profiling of *TFEB* Rearranged and 6p21.1 (*TFEB*) Amplified Tumors

	Tumor Mutation Burden (mt/MB)	Somatic Mutations	Copy Number Changes (Excluding *TFEB*)	Structural Variants
***TFEB* Rearranged Tumors**				
Case 2 *	0.9 mt/MB	*FAT1* p.I2239K	-	*In Frame Fusion: *MALAT1* (Exon1) and *TFEB* (Exon3)
Case 18	0.0 mt/MB	-	-	(*TFEB* rearrangement was detected using FISH)
6p21.1 (*TFEB*) Amplified Tumors				
Case 25	1.0 mt/MB	*NOTCH4* p.S79N	Focal Amplifications: *PIM1*, *CCND3* and *VEGFA* (6p21.1); *SMAD3* and *MAP2K1* (15q22.31) Broad Losses: 3p/6p/8p/15p/16q Broad Gains: 1q/8q/12p/17/20	-
Case 26	8.9 mt/MB	*TP53* p.R273C; *ERRFI1* p.E101V; *LATS2* p.K138N; *LATS2* p.Q148H; *MAP2K1* p.N78S; *MLL2* p.S1484F; *PBRM1* p.F872fs; VHL p.S72fs *SETD2* splicing variant (c. 7432–1G>T);	Focal Gain: *CCND3* (6p21.1) Broad Losses: 2/3p/8p/12p/13q/16q/19/21 Broad Gains: 5q/7/17q	*LATS2* rearrangement: c.1006_1900–1285inv
Case 32	1.8 mt/MB	*RNF43* p.G24V; *STAG2* p.G129R	Focal Amplifications: *CCND3* and *VEGFA* (6p21.1); *RECQL4*, *PRDM14* and *AGO2* (8q24.3) Broad Losses: 2q/8p/20q Broad Gains: 1q/8q/10p/12q/16/17/19/20/21	-
Case 33	5.9 mt/MB	*AKT3* p.W98fs; *AXL* p.K477M; *DNMT3A* p.G642*; *MEN1* p.W126*; *MGA* p.L1003fs; *NTRK3* p.L591V	Focal Amplifications: *CCND3* and *VEGFA* (6p21.1) Broad Losses: 11q/16q/22q Broad Gains: 12p/16q	-
Case 34	3.0 mt/MB	*ASXL1* p.F252I; *EP300* p.H844fs; *YES1* p.D454fs	Focal Amplifications: *PIM1*, *CCND3* and *VEGFA* (6p21.1) Focal Deletions: *E2F3* (6p22.3); *CDKN2B*, *CDKN2Ap16INK4A* and *CDKN2Ap14ARF* (9p21.3) Broad Losses: 2q/6q/17p/18q Broad Gains: 1q/2p/3q/4q/ 5/7/8/11p/12p/14q/16p/17q/19q/20q/22q	-

mt/MB: mutations/megabase; FISH: fluorescence in situ hybridization. The median tumor mutation burden assessed by MSK-IMPACT for all patients with renal cell carcinoma (n=718) is 3.9 mt/Mb.

*Prior Neuroblastoma showed a *PALB2* p.S537L alteration and no germline alterations were detected. *TFEB* rearrangement was detected using FISH and anchored multiplex PCR.

Table2.

Clinicopathologic Features: Case Details

Case No.	Age	Gender	Size (cm)	pT	N	M	Documented Metastasis (At Diagnosis or Follow Up)	Anti-VEGF Therapy	Previously Reported
***TFEB* Rearranged Tumors**									
1	51	Female	14.2	pTx	Nx	Mx	NA	NA	–
2	12	Male	5.4	pT1b	N0	M0	–	NA	–
3	78	Female	3.5	pT1a	N0	M0	–	NA	–
4	49	Female	2	pTx	Nx	Mx	NA	NA	–
5	38	Female	5.3	pTx	Nx	Mx	NA	NA	–
6	59	Female	1.9	pTx	Nx	Mx	NA	NA	–
7	72	Female	4	pT3a	Nx	Mx	NA	NA	–
8	60	Female	4.5	pT1b	Nx	Mx	NA	NA	–
9	68	Male	2.8	pT1a	Nx	Mx	NA	NA	Smith et al, 2014
10	55	Male	9.5	pT3b	Nx	M1	+	NA	–
11	23	Female	3.5	pT1	Nx	Mx	NA	NA	–
12	35	Female	NA	pTx	Nx	Mx	NA	NA	–
13	61	Female	5	pTx	Nx	Mx	NA	NA	–
14	23	Female	NA	pTx	Nx	Mx	NA	NA	–
15	51	Male	14.6	pTx	Nx	Mx	NA	NA	–
16	24	Male	6.4	pT1b	Nx	Mx	NA	NA	–
17	43	Female	10.3	pTx	Nx	Mx	NA	NA	–
18	41	Female	5.8	pT1b	Nx	Mx	–	NA	–
***TFEB* Rearranged Tumors With 6p21.1 (*TFEB*) Amplifications**									
19 (t(6;11) & Amplification)	82	Female	4.5	pT1b	Nx	Mx	NA	NA	–
20 (TCGA-A3-3313-01; *TFEB-KHDRBS2*)	59	Male	4.5	pT1b	Nx	Mx	–	NA	TCGA*
21 (TCGA-B9-A69E-01; *TFEB-CADM2*)	71	Male	8	pT3a	Nx	Mx	–	NA	TCGA*
22 (TCGA-BQ-7048; *COL21A1-TFEB*)	64	Male	11	pT3a	N0	M0	+	+	TCGA*
6p21.1 (*TFEB*) Amplified Tumors									

Case No.	Age	Gender	Size (cm)	pT	N	M	Documented Metastasis (At Diagnosis or Follow Up)	Anti-VEGF Therapy	Previously Reported
23	64	Male	2	pT1a	Nx	Mx	NA	NA	–
24	61	Female	NA	pT3a	Nx	Mx	NA	NA	–
25	23	Female	7	pT1b	Nx	M0	+	NA	Argani et al, 2016
26	53	Male	8.5	pT3a	Nx	M0	+	–	–
27	68	Male	13	pTx	Nx	Mx	NA	NA	–
28	65	Male	NA	pTx	Nx	Mx	NA	NA	Argani et al, 2016
29	66	Female	14	pT3a	Nx	Mx	NA	NA	–
30	78	Female	12	pT3b	Nx	Mx	NA	NA	Argani et al, 2016
31	73	Female	14.4	pTx	Nx	Mx	NA	NA	–
32	73	Male	5	pT1b	Nx	M0	–	NA	–
33	61	Male	13	pT2b	Nx	M1	+	+	–
34	58	Male	9.1	pT3b	N1	M1	+	+	–
35 (TCGA-UZ-A9PQ-01)	59	Male	9.2	pT3a	N1	Mx	+	NA	TCGA *
36 (TCGA-GL-7966–01)	28	Female	6.5	pT3a	N1	Mx	+	NA	TCGA *
37 (TCGA-Q2-A5QZ-01)	61	Female	5.3	pT3a	N0	Mx	+	NA	TCGA *

* The Cancer Genome Atlas (TCGA) cases have been reported in multiple studies including: Malouf et al, (14); TCGA Research Network, (15); Argani et al, (2); Williamson et al, (8); Gupta et al, (9); Mendel et al, (12); Calio et al, (11).

Table3.

Clinicopathologic Features: Summarized Data

	***TFEB* Rearranged Tumors**	***TFEB* Rearranged Tumors With 6p21.1 (*TFEB*) Amplifications**	**6p21.1 Amplified Tumors**	**All *TFEB* Altered tumors**
Total Number of Cases	22 *	4 **	15	37
Age < 25 years	4/22 (Mean: 51years)	0/4 (Mean: 58years)	1/15 (Mean: 59years)	5/37 (Mean: 54years)
Gender (Male: Female)	8:14	3:1	8:7	16:21
Size (mean, cm)	**6.3 (n=20)**	6.4 (n=4)	**9.2 (n=13); *p*=0.04**	7.4 (n=33)
≥pT3	4/13 (31%)	2/4	8/11 (73%); *p*=0.1	12/24
N1	0/3	0/2	1/3	3/7
M1	2/4	1/1	2/5	4/9
Documented Distant/ Regional Metastasis at Diagnosis or Follow Up	**2/7 (29%)**	1/3	**7/8 (88%); *p*=0.04**	9/15
Anti-VEGF Therapy	Documented in 1 Case	Documented in 1 Case	Documented in 2 Cases	Documented in 3 Cases

VEGF: Vascular Endothelial Growth Factor

* Rearrangement partners include *MALAT1* (n=19), *COL21A1* (n=1), *CADM2* (n=1) and *KHDRBS2* (n=1).

** Rearrangement partners include *MALAT1* (n=1), *COL21A1* (n=1), *CADM2* (n=1) and *KHDRBS2* (n=1).

Statistical analysis performed using Fishers exact test.

Table4.

Methods & Histopathology: Case Details

Case No.	Digital PCR (*TFEB*/ *B2M* Percentage)	IHC: TFEB	IHC: CathepsinK/ MelanA/ HMB45	Morphology	Biphasic Features	Cytoplasmic Features	WHO/ISUP Grade	Sarcomatoid/Rhabdoid Features/Coagulative Necrosis	Pigment/ Calcifications
***TFEB* Rearranged Tumors**									
1	2.4	NA	CathepsinK^{+}, MelanA^{+}, HMB45^{+}	Tubulopapillary	−	Eosinophilic	3	Necrosis^{+}	−
2	148.9	+	CathepsinK^{+}	Acinar	+	Clear	3	−	−
3	297.8	+	CathepsinK^{+}	Solid	+	Clear	3	−	−
4	313.2	NA	CathepsinK^{+}, MelanA^{+}, HMB45^{-}	Nested	−	Clear	2	−	−
5	124.4	NA	CathepsinK^{+}, MelanA^{+}, HMB45^{+}	Acinar	+	Clear	2	−	−
6	196	NA	CathepsinK^{+}, MelanA^{+}	Nested	+	Clear	2	−	Calcification^{+}
7	2.9	+	CathepsinK^{+}, MelanA^{+}, HMB45^{+}	Tubulopapillary	−	Eosinophilic	4	Sarcomatoid^{+}	Pigment^{+}
8	46.4	+	CathepsinK^{+}	Tubulopapillary	−	Eosinophilic	2	−	−
9	38.6	+	CathepsinK^{+}, MelanA^{+}	Solid	−	Clear	2	−	−
10	34.8	+	CathepsinK^{+}	Nested	−	Clear	3	Necrosis^{+}	−
11	632.1	NA	CathepsinK^{+}, MelanA^{+}, HMB45^{+}	Nested	+	Clear	4	Rhabdoid^{+}	−
12	76.2	NA	CathepsinK^{+}, HMB45^{+}	Other	−	Clear	1	−	−
13	26.2	NA	CathepsinK^{+}	Tubulopapillary	−	Clear	2	Necrosis^{+}	−
14	217.3	NA	CathepsinK^{+}, MelanA^{+}	Acinar	+	Clear	2	−	−
15	40.9	NA	CathepsinK^{+}, MelanA^{+}, HMB45^{-}	Solid	−	Clear	2	−	Calcification^{+}
16	804.2	NA	CathepsinK^{+}, MelanA^{+}	Solid	+	Clear	1	−	−
17	890	NA	CathepsinK^{+}, MelanA^{+}, HMB45^{+}	Nested	+	Clear	1	−	Pigment^{+}, Calcification^{+}
18	NA	+	CathepsinK^{+}, MelanA^{+}	Solid	−	Clear	2	−	−
***TFEB* Rearranged Tumors With 6p21.1 (*TFEB*) Amplifications**									
19 (t(6;11) & Amplification)	72.7	NA	CathepsinK^{+}, MelanA^{+}, HMB45^{-}	Nested	−	Eosinophilic	3	Necrosis^{+}	−
20 (TCGA-A3-3313-01; *TFEB-KHDRBS2*)	NA	NA	NA	Nested	−	Clear	3	NA	NA
21 (TCGA-B9-A69E-01; *TFEB-CADM2*)	NA	NA	NA	Tubulopapillary	−	Eosinophilic	2	NA	−
22 (TCGA-BQ-7048; *COL21A1-TFEB*)	304.3	+	NA	Tubulopapillary	+	Eosinophilic	3	−	Calcification^{+}
6p21.1 (*TFEB*) Amplified Tumors									

Case No.	Digital PCR (*TFEB*/ *B2M* Percentage)	IHC: TFEB	IHC: CathepsinK/ MelanA/ HMB45	Morphology	Biphasic Features	Cytoplasmic Features	WHO/ISUP Grade	Sarcomatoid/Rhabdoid Features/Coagulative Necrosis	Pigment/ Calcifications
23	3.7	NA	CathepsinK^{+}, MelanA^{+}, HMB45^{-}	Tubulopapillary	−	Eosinophilic	3	−	−
24	82.2	NA	CathepsinK^{+}, MelanA^{+}, HMB45^{-}	Tubulopapillary	−	Eosinophilic	4	Necrosis^{+}, Rhabdoid^{+}	Pigment^{+}
25	169.8	NA	NA	Nested	−	Eosinophilic	4	−	−
26	29.6	−	NA	Nested	−	Clear	4	Necrosis^{+}, Sarcomatoid+	−
27	10.5	NA	CathepsinK^{+}, MelanA^{+}, HMB45^{+}	Tubulopapillary	−	Eosinophilic	3	−	−
28	85.4	NA	CathepsinK^{+}, MelanA^{+}, HMB45^{-}	Nested	−	Eosinophilic	3	−	−
29	7.9	NA	CathepsinK^{-}, MelanA^{-}, HMB45^{-}	Nested	−	Clear	3	Necrosis^{+}	−
30	66.5	+ (weak)	CathepsinK^{+}, MelanA^{+}, HMB45^{-}	Tubulopapillary	−	Eosinophilic	3	Necrosis^{+}	−
31	5.3	NA	MelanA^{+}, HMB45^{-}	Solid	−	Eosinophilic	3	Necrosis^{+}	−
32	NA	NA	NA	Tubulopapillary	−	Eosinophilic	3	−	−
33	NA	NA	NA	Papillary	−	Eosinophilic	3	−	−
34	NA	NA	NA	NA	NA	NA	NA	−	NA
35 (TCGA-UZ-A9PQ-01)	NA	NA	NA	Other	−	Eosinophilic	3	NA	NA
36 (TCGA-GL-7966–01)	NA	NA	NA	Tubulopapillary	−	Eosinophilic	3	NA	NA
37 (TCGA-Q2-A5QZ-01)	NA	NA	NA	Papillary	−	Eosinophilic	3	Necrosis^{+}	NA

Table5.

Methods & Histopathology: Summarized Data

	***TFEB* Rearranged Tumors**	***TFEB* Rearranged Tumors With 6p21.1 (*TFEB*) Amplifications**	**6p21.1 (*TFEB*) Amplified Tumors**	**All *TFEB* Altered tumors**
Total Number of Cases	22 *	4 **	15	37
Digital PCR (*TFEB*/*B2M* > 20%)	**17/19 (90%)**	2/2	**5/9 (56%); *p*=0.06**	22/28 (78.6%)
Immunohistochemistry (Diffuse Positivity: TFEB)	8/8 (100%)	1/1	1/2 (50%) (weak staining)	9/10 (90%)
Immunohistochemistry (CathepsinK/ MelanA/ HMB45)	19/19 (100%)	1/1	6/7 (85.7%)	25/26 (96%)
Morphology: Papillary	0/22 (0%)	0/4	2/14 (14.2%); *p*=0.14	2/36 (5.5%)
Morphology: Tubulopapillary	6/22 (27.3%)	2/4	6/14 (42.8%); *p*=0.47	12/36 (33.3%)
Morphology: Solid	5/22 (22.7%)	0/4	1/14 (7.1%); *p*=0.37	6/36 (16.7%)
Morphology: Nested	7/22 (31.8%)	2/4	4/14 (28.6%); *p*=1.0	11/36 (30.5%)
Morphology: Acinar	3/22 (13.6%)	0/4	0/14 (0%); *p*=0.27	3/36 (8.3%)
Morphology: Biphasic Features	**9/22 (41%)**	1/4	**0/14 (0%); *p*=0.006**	9/36 (25%)
Cytoplasm: Predominantly Eosinophilic	**6/22 (27.3%)**	1/3	**12/14 (85.7%); *p*=0.0016**	18/36 (50%)
Cytoplasm: Predominantly Clear	**16/22 (72.7%)**	1/4	**2/14 (14.3%); *p*=0.0016**	18/36 (50%)
≥WHO/ISUP Grade3	**9/22 (41%)**	1/3	**14/14 (100%); *p*=0.0003**	23/36 (63.8%)
Rhabdoid Features	Documented in 1 Case	-	Documented in 1 Case	Documented in 2 Cases
Sarcomatoid Features	Documented in 1 Case	-	Documented in 1 Case	Documented in 2 Cases
Coagulative Necrosis	Documented in 4 Cases	Documented in 1 Case	Documented in 6 Cases	Documented in 10 Cases
Pigment	Documented in 2 Cases	-	Documented in 1 Case	Documented in 3 Cases
Calcification	Documented in 4 Cases	Documented in 1 Case	-	Documented in 4 Cases

WHO: World Health Organization; ISUP: International Society of Urologic Pathology

* Rearrangement partners include *MALAT1* (n=19), *COL21A1* (n=1), *CADM2* (n=1) and *KHDRBS2* (n=1).

** Rearrangement partners include *MALAT1* (n=1), *COL21A1* (n=1), *CADM2* (n=1) and *KHDRBS2* (n=1).

Statistical analysis performed using Fishers exact test.

Table6.

Reports of Regional and Distant Metastasis in Tumors with Molecular Confirmation of 6p21.1 (*TFEB*) Amplification or *TFEB* Rearrangement

***TFEB* Rearranged Tumors**		**6p21.1 Amplified Tumors (With or Without *TFEB* Rearrangements)**	
Reference	**Total Cases**	**Reference**	**Total Cases**
Pecciarini et al, 2007	1	Peckova et al, 2014	1
Camparo et al, 2008	1	Argani et al, 2016	4
Ishihara et al, 2011	1	TCGA Malouf et al, 2014 TCGA Research Network, 2016 Argani et al, 2016 Williamson et al, 2017 Gupta et al, 2017 Mendel et al, 2018 Calio et al, 2018	4
Argani et al, 2012	2	Gupta et al, 2017 *	5
Inamura et al, 2012	1	Qu et al, 2017	1
Smith et al, 2014	1	Skala et al, 2017	2
Hora et al, 2014	1	Mendel et al, 2018	3
Lilleby et al, 2015	1	Calio et al, 2018 *	1
Calio et al, 2017	2	Kojima et al, 2019	1
Kojima et al, 2019	1	Current study	3
Current Study	1		
Total Cases (1996 to 2019)	**13 (≈12.3%)**	**Total Cases (2014 to 2019)**	**25 (≈43.9%)**
Approximate Total Number of Reported Cases	**106**	**Approximate Total Number of Reported Cases**	**57**

* 8 of 16 (≈50%) cases with low level gains exhibited regional or distant metastasis. TCGA: The Cancer Genome Atlas.